Re-analysis of surface piercing propellers performance data

M.A. Kotb
Marine Eng. and Naval Architecture Dept., Alexandria University, Alexandria, Egypt
E-mail: Kotb2000@yahoo.com

In recent years, an increasing number of high-speed yachts and patrol boats have been propelled by Surface Piercing Propellers (SPP). This was due to the several attractive advantages offered by this type of propellers. These are manifested in unrestricted propeller diameter, minimum appendage drag, and excellent cavitation performance. The performance of this type of propulsion is influenced by some extra factors which do not exist in case of conventional (fully submerged) propellers. These factors are shaft inclination angle, immersion area, and Weber's number. In this work, the test results of model testing of SPPs are expressed in different notations which reflect the new parameters involved. A new design chart is also developed to help determine diameter, pitch, and efficiency of surface piercing propellers under different loading conditions.

في السنوات القليلة الماضية حدث نمو مضطرد في استخدام الرفاصات البحرية المغمورة جزئيا (والتي تكون أعمدة إدارتها وجزء كبير من أقطارها خارج المياه) في تسيير ودفع المركبات البحرية السريعة والسبب المباشر لهذا هو المزايا العديدة لتلك الرفاصات ومنها إمكانية استخدام أقطار أكبر مع نقص ملحوظ في الإعاقة الناشئة عن ملحقات السفن وخصوصا عند السرعات العالية كذلك الأداء الجيد لتلك الرفاصات بالنسبة لظاهرة التكهف. يعتمد أداء هذه الرفاصات علي بعض العوامل التي لا تؤثر علي الرفاصات التقليدية والتي تكون في حالة غمر كلي و تتمثل تلك العوامل في ميل أعمدة الإدارة وتغير مساحة الجزء المغمور من قرص الرفاص وكذلك تأثير التوتر السطحي للماء علي تغلل الهواء حول قرص الرفاص أثناء دخول وخروج العنفات من والي سطح الماء. يتناول هذا البحث طريقة عرض نتائج أداء الرفاصات المغمورة جزئيا سواء المعملية أو النظرية وضرورة وضعها في شكل يبرز خصوصية عمل تلك الرفاصات كذلك تم اقتراح بعض الخرائط التي تحتوي نتائج الاختبارات المعملية لمجموعة أو سلسلة من تلك الرفاصات والتي يمكن عن طريقها تصميم رفاص ليناسب قارب سريع أو تقييم أداء رفاص موجود عند أحمال تشغيل مختلفة.

Keywords: Surface piercing propellers, SPP, Propeller design chart, Surface drive, Partially submerged propellers

1. Introduction

A surface-piercing propeller is classified among unconventional propulsor family because of its particular mode of operation. [1]. It operates at partially submerged conditions where the propeller shaft is extended out through the transom of the vessel; fig. 1. Blade sections, as well as, outline are shaped differently from conventional propellers. Sharp leading edges, straight trailing edges, wedge or concave sections are typical features in surface propellers.

Propulsion systems utilizing surface piercing propellers are classified in two main groups. These are fixed and articulated systems. The former is more simple while the later needs some what complicated mechanism. Fig. 2 displays the main features of each group.

Surface-piercing propellers possess a number of attractive advantages over submerged propellers. Appendage drag due to shafts, struts, propeller hub, etc. are very much reduced if not eliminated. Propeller size is not limited by blade tip clearance from the hull or maximum vessel draft and hence larger propellers can be used which is reflected positively on higher propulsive efficiency. Finally, blade surface erosion caused by cavitation are largely reduced.

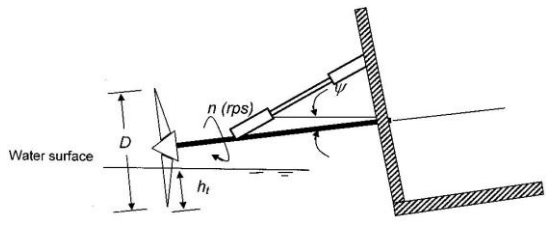

Fig. 1. Surface piercing propeller.

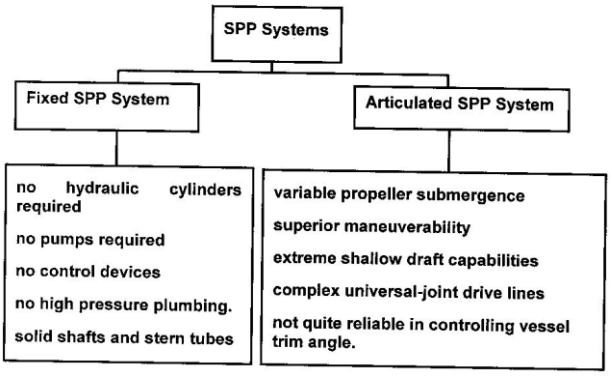

Fig. 2. Surface pierce propulsion systems.

Surface Piercing Propeller proved to be a very efficient propulsion device for high speed shallow draft crafts. Each of the other propulsion devices in use for high speed crafts has its own drawbacks. Conventional propellers suffer from cavitation at high speeds. Super cavitating propellers on the other hand exhibit high appendage drag. Waterjets and the associated duct configurations have relatively heavy installations weight.

A number of model testing was carried out to measure the performance of surface piercing propellers in free surface tunnels and/or towing tanks. Examples include [2-4], and [5]. Other tests, measuring propeller thrust and torque, together with vertical and horizontal forces and moments are also carried out and reported in [6,7] and [8].

Ferrando et al. [9] have tested a series of surface piercing propellers and experimentally investigated the influence of Weber's number on transition. They also proposed modified torque and thrust coefficients based on immersed area.

Numerical analysis of surface piercing propellers have been done by several researchers using different approaches varying in the level of sophistication. Oberembt [10] used a lifting line model assuming no natural ventilation of the propeller. Furuya [11] included ventilation in his lifting line approach. Kinnas et. al. [12] developed a 2D time marching panel method to analyze the flowfield around and past partially submerged propellers.

Due to the impeded limiting assumptions and simplifications in these numerical analysis regarding flow aspects associated with surface piercing propeller operation, one still has to rely on experimental results.

Unlike conventional propellers, very few surface piercing propellers systematic data exist. These are incomplete, scattered, and are not presented in such a way to reflect significant operating parameters. Hence, it is very much recommended to document the little scattered data and present them in a useful form suitable for practical design, and performance assessments.

The objective of the current work is to re-examine the existing data of surface piercing propeller model tests and present such data in different forms which better reflect the particular operating aspects involved. Also, diagrams and charts are prepared and suggested for use in design and prediction of the performance of surface-piercing propellers.

Table 1 gives a summary of available test results on surface piercing propellers. It is to be noted that some of the test conditions and/or geometrical particulars are not reported or just missing.

2. Performance analysis

Curves presenting open water performance for surface piercing propellers look quite different from conventional propellers. Typical thrust coefficient K_T versus advance coefficient J curve for fully and partially submerged propellers are shown in fig. 3. It can be seen that static thrust for SPP's and partially submerged propellers is much less than conventional propellers. At low values of advance coefficient the surface piercing propeller behaves in an opposite trend to conventional propeller. The $K_T - J$ curve is characterized by a sudden thrust increase at a particular J value. This value was found to be a function of both immersion ratio and Weber's number. It actually occurs between two regions of operations; namely base vented and fully vented [13].

The advance coefficient J where complete ventilation takes place is termed the critical advance coefficient J_{CR}. At this value, both thrust and torque coefficient of SPP exhibit discontinuities; see fig. 4.

Table 1
Summary of available test results on surface piercing propellers

Series name	No. of blades	BAR	P/D	Immersion ratio (I_T)	Inclination angle (ψ)
Rolla (8)	4	0.8	0.9 1.1 1.2 1.4 1.6	0.47	8^0
VeemSurf (16)	3 4 5	0.45 0.60 0.75	0.85 To 1.25	-	-
L4.68 (13)	4	0.68	0.8 1.0 1.2 1.4	0.4 0.5 0.6 0.7	4^0 6^0 8^0
CP372(2)	5	0.72	1.19	0.3 0.4 0.5	-
Teignbridge propellers (6)	4 5	-	1.50	0.3 0.5 0.8	-

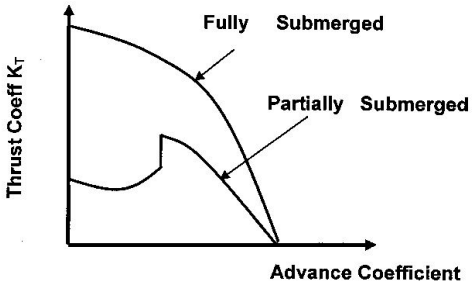

Fig. 3. Open water thrust curves for fully and partially submerged propellers.

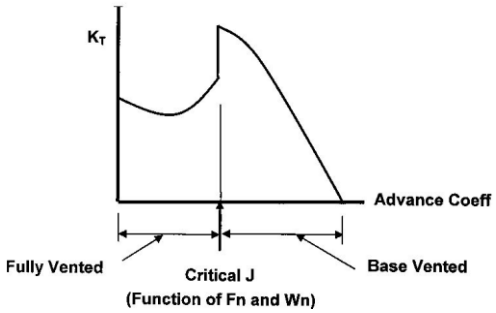

Fig. 4. Typical thrust speed curve for SPP's.

To understand the reasons behind such different performance pattern, it was necessary to look at the factors affecting such performance. For surface piercing propellers thrust, torque coefficients, and hence efficiency are functions of a number of geometrical and operational parameters. These are number of blades, pitch ratio, blade area ratio, shaft yaw and pitch angles, immersion ratio, advance coefficient, Reynold's, Froude's and Weber's numbers. Immersion ratio and Weber's numbers are particular factors in case of surface piercing propellers due to their special mode of operation.

The influence of the number of blades, pitch ratio, blade area ratio and advance coefficient on the behavior of a surface piercing propellers is much the same as in the case of fully immersed propellers. The same is true for the Reynold's number.

The influence of Froude's number is relevant as the propeller acts at the interface between air and water much like hulls. The influence of *Fn* based on the diameter of the propeller as the length parameter and *nD* as the speed, vanished when the air cavity approaches its ultimate form, i.e. for Froude's numbers greater than 3 [14], and greater than 4 [2] as limiting values beyond which the influence disappears. Hence, provided that open water tests are performed at *Fn* beyond the threshold values, the Froude's number identity can be avoided during the tests without affecting the full scale performance of the propeller.

According to [14], surface tension plays its role when the propeller is about to be fully

ventilated. Complete ventilation is a rather sudden phenomenon that can be correlated to a particular value of *J;* namely J_{CR}. The critical advance coefficient can roughly be located in the middle of the transition region and the sudden drop of K_T and K_Q identify its position. Correlation between Weber's numberand J_{CR} for surface piercing propellers was studied in [9] and [14]. The threshold value depends on the form of Weber number used.

Depending on the form of Weber's number, experimental work showed that there is also a threshold value beyond which the performance of SPP is not affected by Weber's number. Table 2 shows these threshold values where k is the fluid kinematic capilarity.

As far as known, provided that open water tests are performed in agreement with the above requirements, the performance of SPPs can be scaled in the same fashion as conventional propellers, i.e. by applying a Reynolds number correction only.

The immersion coefficient I_T is the ratio between the maximum blade tip immersion h_t and the propeller diameter D and the value of this coefficient indicates how much of the propeller is working under water. It is defined as follows:

$$I_T = \frac{h_t}{D}. \tag{1}$$

The immersion ratio h_t/D is related to submerged area ratio A_0/D^2 as:

$$\frac{A_0}{D^2} = 0.25\cos^{-1}(1-2I_T) - (0.5-I_T)\sqrt{I_T(1-I_T)} \quad I_T \le 1.0. \tag{2}$$

I_T = 1.0 indicates that the propeller is fully immersed. The corresponding submerged area ratio is $\pi/4$, see fig. 5. I_T is the most significant parameter that indicates whether the propeller is fully or partially submerged.

Table 2
Threshold values

Weber's number form	Threshold value
$\sqrt{\frac{n^2D^3}{k}}$	180
$\sqrt{\frac{n^2D^2h_t}{k}}$	270

Propeller thrust, torque, speed and open water efficiency are generally presented in non dimensional forms as:

$$K_T = \frac{T}{\rho n^2 D^4} \quad K_Q = \frac{Q}{\rho n^2 D^5}$$
$$J = \frac{V_A}{nD} \quad \eta = \frac{K_T}{K_Q}\frac{J}{2\pi}. \tag{3}$$

For propellers working at varying values of immersion ratios I_T and shaft inclinations, ψ it is necessary to redefine the above coefficients in such a way to include both parameters. A form suggested by Fernando (9) is given as:

$$K_T' = \frac{T}{\rho n^2 D^2 A_0} \quad K_Q' = \frac{Q}{\rho n^2 D^3 A_0}$$
$$J' = \frac{V_A \cos(\psi)}{nD} \quad \eta' = \frac{K_T'}{K_Q'}\frac{J'}{2\pi}. \tag{4}$$

The new forms of coefficients are still non dimensional and are related to conventional form as:

$$K_T' = \frac{K_T}{0.25\cos^{-1}(1-2I_T) - (0.5-I_T)\sqrt{I_T(1-I_T)}}$$
$$K_Q' = \frac{K_Q}{0.25\cos^{-1}(1-2I_T) - (0.5-I_T)\sqrt{I_T(1-I_T)}}$$
$$J' = J\cos(\psi) \qquad \eta' = \eta\cos(\psi). \tag{5}$$

It was found out that when using these modified coefficients, the results for a propeller tested at different values of immersion ratios collapse into one single curve for advance coefficient greater than J_{CR}. Fig. 6 shows that K_T is dependent on immersion ratio while K'_T is not. Hence, the curves K'_T and K'_Q versus J'. are independent of the immersion of the pro peller. Below the transition this is no longer true.

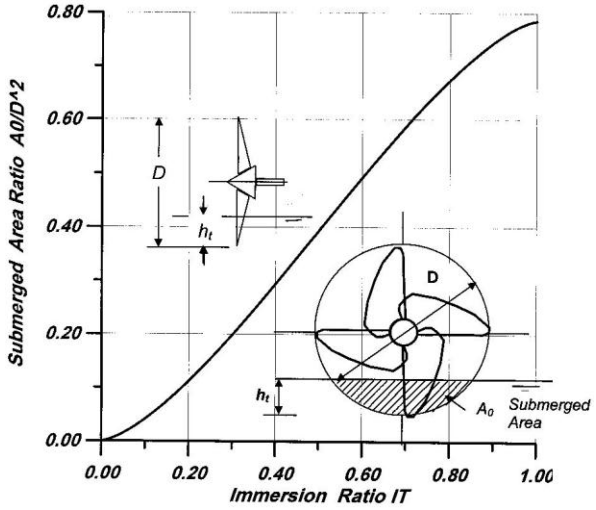

Fig. 5. Submerged area ratio versus immersion ratio.

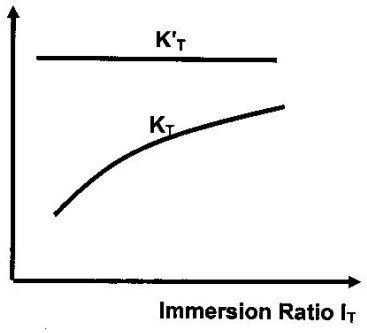

Fig. 6. K_T and K'_T dependence on propeller immersion ratio.

3. Design charts

Expressing the absorbed torque Q in terms of delivered power P_D and propeller rotational speed n as:

$$Q = \frac{P_D}{2\pi n}. \tag{6}$$

Propeller diameter D is also expressed in terms of speed of advance V_A, shaft angle ψ, and propeller rotational speed n as:

$$D = \frac{V_A \cos\psi}{nJ'}. \tag{7}$$

Substituting eqs. (6) and (7) into the torque coefficient equation K'_Q definition given in eq. (4):

$$K'_Q = \frac{P_D n^2 J'^5}{2\rho\pi (V_A \cos\psi)^5 \left(\frac{A_0}{D^2}\right)}. \tag{8}$$

Rearranging eq. (8) and taking the square roots of both sides:

$$\sqrt{2\rho\pi}\sqrt{\frac{K_Q'}{J'^5}} = \frac{\sqrt{P_D}\,n}{(V_A \cos\psi)^{2.5}}\sqrt{\left(\frac{D^2}{A_0}\right)}. \tag{9}$$

The term on the right hand side of eq. (9) is defined as propeller power coefficient Bp' which doesn't include propeller diameter. The term (D^2/Ao) is just related to immersion ratio I_T.

$$B'_P = \frac{\sqrt{P_D}\,n}{(V_A \cos\psi)^{2.5}}\sqrt{\left(\frac{D^2}{A_0}\right)} = \sqrt{2\rho\pi}\sqrt{\frac{K'_Q}{J'^5}}. \tag{10}$$

To emphasize that the power coefficient is independent on propeller diameter the immersion ratio (Ao/D^2) from eq. (2) is substituted into eq. (10);

$$B'_P = \frac{\sqrt{P_D}\,n}{(V_A \cos\psi)^{2.5}\sqrt{0.25\cos^{-1}(1-2I_T) - (0.5-I_T)\sqrt{I_T(1-I_T)^2}}} = \sqrt{2\rho\pi}\sqrt{\frac{K'_Q}{J'^5}}. \tag{11}$$

The introduced propeller power coefficient Bp' includes, in addition to delivered power, speed of advance, and propeller rotation, the immersion ratio and shaft inclination. It is also related to torque and advanced coefficient as:

$$B'_P = 33.2\sqrt{\frac{K'_Q}{J'^5}}. \tag{12}$$

The constant here is inserted to permit using horsepower, knots, and rpm for P_D, V_A, and n. For the purpose of surface piercing propeller design and selection, the power coef-

ficient is presented as a function of pitch ratio P/D, open water η efficiency, and advance coefficient J' for a family of propellers which can be used as in a similar way to conventional propellers or as a tool handy for design.

Two cases of SPP experimental results shown in table 3 will be presented in the new format. Furthermore, design charts for each propeller family is developed. These charts will be used to design a surface piercing propeller as illustrated through a numerical example.

4. Case study (1)

Model test results of this propeller family are given in (9) and presented in the K'_T, K'_Q, J', and η' parameters for advance coefficient values passed the critical J' values in figs. 7, 8, and 9 respectively. Locus of critical advance coefficient were plotted on the same graphs. These data are further reduced to sets of open water efficiency and advance coefficient contours plotted on a grid of pitch diameter ratio, P/D and power coefficient Bp' parameters as shown in fig. 10. A maximum efficiency and critical advance coefficient lines are also displayed on the same plot.

5. Case study (2)

This case is a 4-bladed surface piercing propeller series designed by Rolla tested at one immersion ratio (I_T = 0.47) at a single shaft inclination value ψ = 8°. The test results are reported in [8] in conventional K_T, K_Q, J, and η format. Making use of the fact that thrust and torque results for all immersions collapse into one single curve for advance coefficient J' values passed the critical one, the

Table 3

Case	1	2
Reference	(13)	(8)
Series	L468	Rolla
No of blades	4	4
Blade area ratio	0.68	0.8
Immersion ratio	0.4,0.5,0.6,0.7	0.47
Pitch ratio P/D	0.8,1.0,1.2,1.4	0.9,1.1,1.2,1.4,1.6
Yaw angle (deg)	0	0
Shaft inclination (deg)	4, 6, 8	8

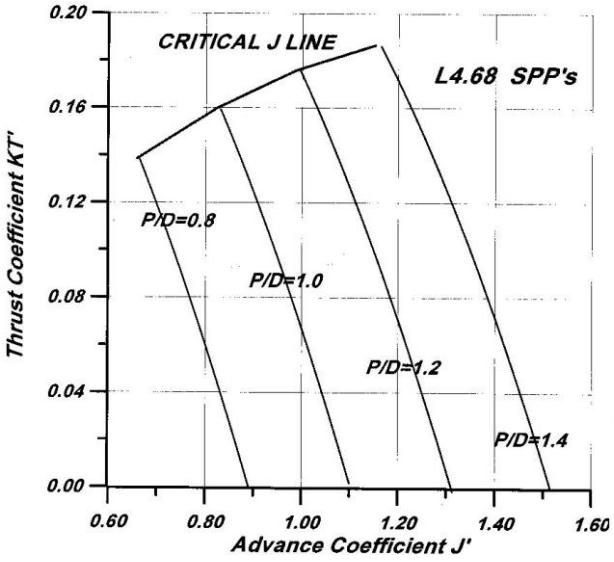

Fig. 7. Thrust coefficient K'_T versus advance coefficient J' for the L4. 68 surface piercing propeller series.

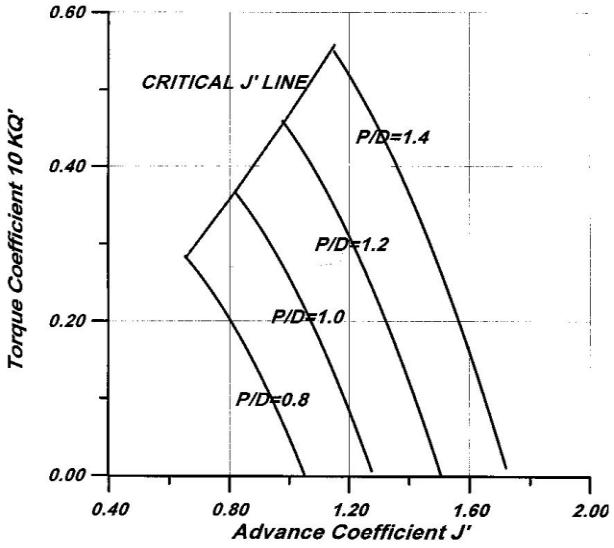

Fig. 8. Torque coefficient K'_Q versus advance coefficient J' for the L4. 68 surface piercing propeller series.

original data is converted into modified sets of data; namely K'_T, K'_Q, J', and η'. Fig. 11 shows the thrust coefficient K'_T versus J' for this propeller family. The location of critical J was determined for each P/D by examining the K_T - J curve and locating the advance coefficient at which thrust coefficient starts to drop. The critical J value was also determined making use of the Weber's number dependence as given in [9] and [14]. The thrust and efficiency

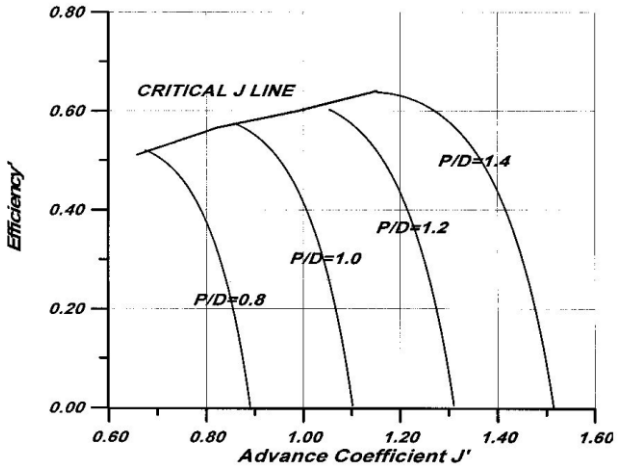

Fig. 9. Efficiency versus advance coefficient J' for the L4. 68 surface piercing propeller series.

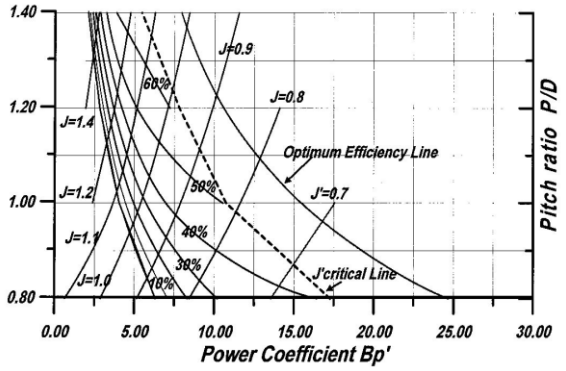

Fig. 10. Thrust coefficient Bp' – J' diagram for the L4.68 surface piercing propeller series.

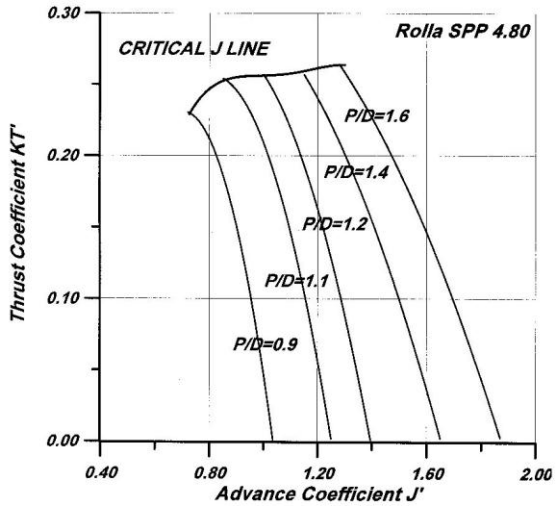

Fig. 11. Thrust coefficient K'_T versus advance coefficient J' for the Rolla surface piercing propeller series.

values corresponding to critical advance coefficients at each pitch ratio are given on fig. 12. The above results are used to prepare another design chart given in fig 13. On this chart a maximum efficiency line is plotted together with another line or locus for points of critical advance coefficient. The chart can be used to assist the design process of surface-piercing propellers. It can also be used to examine the effect of operating at different immersion ratios.

6. Example to illustrate the use of the developed charts

The new developed charts for the L4.68 and Rolla surface piercing propeller series are used here to design a propeller that fits to a high-speed craft with an overall length of 20 meters and a maximum speed of 42 knots. [15]. Other particulars for the boat are given in table 5.

Thrust deduction and wake fraction are typically zero for the intended boat propellers as they are extended out and away from hull

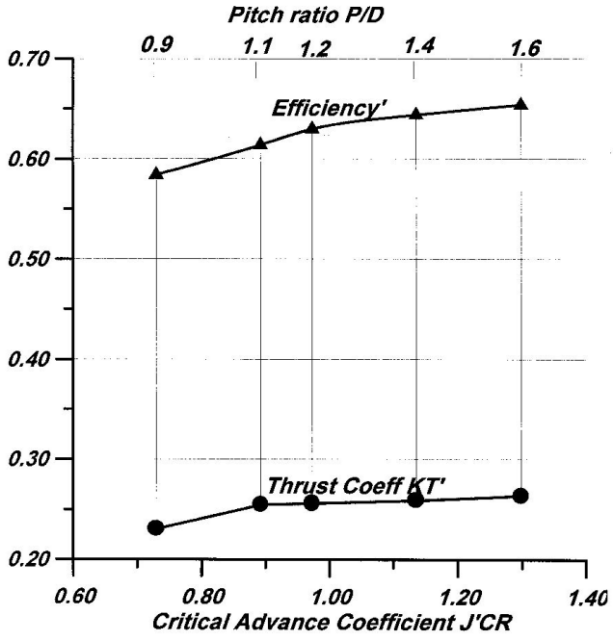

Fig. 12. Values of thrust coefficient K'_T and open water efficiency η' at critical advance coefficient for the Rolla surface piercing propellers.

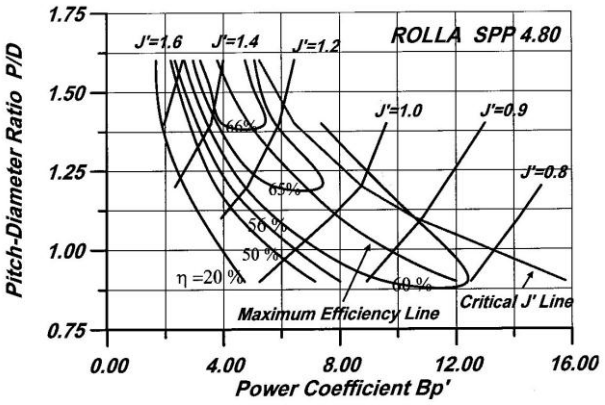

Fig. 13. Thrust coefficient Bp' – J' diagram for the Rolla surface piercing propeller series.

Table 5
Particulars for the boot

Length (m)	20.0
LWL (m)	17.3
Breadth (m)	5.0
Depth (m)	2.80
Draft (m)	0.92
Weight (ton)	35.6
Installed power (hp)	1420 x 2 @2300 rpm
Reduction ratio	1.524:1
Expanded Blade Area Ratio	0.8
Wake fraction	0
Thrust deduction	0
No of Blades	4
Speed (knot)	42.0
Total Resistance (kN) @ 42 knots	56.41

stern. The boat is moving in a planning mode as indicated from the volumetric Froude's number $Fn_{\nabla} = \frac{V}{\sqrt{g\nabla^{1/3}}} = 3.82 > 2.5$ and Length Froude's number $Fn_L = \frac{V}{\sqrt{gL}} = 1.685$. The total boat resistance as calculated from the model tests (and accounting for appendages, air, and wave resistance) is 56.41 KN at V_S=42 knots. Hence, the effective power is 1218.726 kw. Assuming an overall propulsive coefficient of 0.60, the delivered power is estimated to be 2031.2 kw. (2708.2 hp). Assuming 5% mechanical and gear box losses the installed power will be 2850 hp which is quite close to the actual installed power.

To use the proposed developed charts one needs to know the power coefficient Bp' which is calculated from:

$$B_P^{'} = \frac{n\sqrt{P_D}}{(V_A \cos\varphi)^{2.5}} \sqrt{\frac{D^2}{A_0}}, \qquad (13)$$

, a shaft angle of 8 degrees and a 0.5 immersion ratio (Ao/D^2=0.3927) are assumed. Hence B_P'= 10.89.

From or the two developed charts we get the outputs given in table 6.

Checking the resulting Quasi Propulsive Coefficient (QPC) where relative rotative efficiency is nearly one and hull efficiency is typically one (which will be exactly the open water efficiency) we get 0.62 and 0.65 which are quite close to the assumed value of (0.60).

7. Conclusions

The main conclusions that can be drawn from this work are as follows:

- The effects of both Froude's and Weber's numbers can be ignored if the open water tests of surface piercing propeller are performed at values beyond the thresholds mentioned above.
- Open water test results of the surface piercing propellers should be presented in such a way to significantly reflect their geometrical and operational parameters as illustrated in this work.
- The modified thrust and torque coefficients K_T', K_Q' J', and η' are independent of the

Table 6
Outputs

Parameter	*I*4.68 design chart	Rolla design chart
Pitch/diameter ratio P/D	0.98	0.95
Advance coeff J	0.88	0.82
Propeller efficiency η'	0.65	0.62
Diameter D	0.985	1.037
Quasi propulsive coefficient.	0.65	0.62

propeller immersion for values of the advance coefficient greater than the critical value.

• Further research work is needed on SPPs to assess the influence of other parameters, such as number of blades, blade area ratio, the rake angle, and the shaft inclinations on the overall performance and on side and vertical forces.

Nomenclature

A_0 is the propeller submerged area,
BAR is the propeller blade area ratio,
Bp' is the propeller power coefficient $= \frac{n\sqrt{P_D}}{(V_A \cos\varphi)^{2.5}} \sqrt{\frac{D^2}{A_0}}$,
D is the propeller diameter,
Fn_∇ is the volumetric Froude's number $= V/\sqrt{g\nabla^{1/3}}$,
Fn_L is the length Froude's number $= V/\sqrt{gL}$,
h_t is the blade tip immersion,
I_T is the immersion ratio coefficient $= h_t/D$,
J is the advance coefficient $= V_A/nD$,
J' is the modified advance coefficient $= V_A \cos(\psi)/nD$,
J_{CR} is the critical advance coefficient
k is the fluid kinematic capilarity
K_T is the thrust coefficient $= T/\rho n^2 D^4$,
K'_T is the modified thrust coefficient $= T/\rho n^2 D^2 A_0$,
K_Q is the torque coefficient $= Q/\rho n^2 D^5$,
K'_Q is the modified torque coefficient $K_{Q'} = Q/\rho n^2 D^3 A_0$,
L is the ship's length,
n is the propeller rotational speed ,
P is the propeller pitch,
P_D is the delivered power,
Q is the absorbed torque,
QPC is the quasi propulsive coefficient,
Rn is the Reynolds number,
T is the propeller thrust,
V_A is the speed of advance,
W is the Weber's number see table 3,
η is the propeller open water efficiency $= K_T J/2\pi K_Q$,
η' is the propeller open water efficiency $= K_T' J'/2\pi K_Q'$,
ρ is the water density,
ψ is the shaft yaw angle , and
∇ is the volume of displacement.

References

[1] The Specialist Committee on Unconventional Propulsors Final Report and Recommendations to the 22nd ITTC (1999).

[2] W. Miller, and J. Szantyr, "Model Experiments with Surface Piercing Propellers", Ship Technology Research, Vol. 45 (1998)

[3] Y. Shen, "General Scaling Problems on Fully Cavitating and Ventilated Flows", the 17th ATTC, Pasadena, USA (1975).

[4] Scherer, "Partially Submerged and Supercavitating Propellers", the 18th ATTC, Annapolis, USA (1977).

[5] J.B. Hedler, and R. Hecker "Performance of Partially Submerged Propellers", Proceedings of the Seventh Symposium on Naval Hydrodynamics, Rome, Italy (1968).

[6] J. Chudley, D. Grieve, and P.K. Dyson, "Determination of Transient Loads on Surface Piercing Propellers", Trans RINA, (2003).

[7] J.C. Rose, and C.F.L. Kruppe, and K. Koushan, "Surface Piercing Propellers – Propeller Hull Interaction", Proceeding Fast'93, Yokohama, Japan, Vol. 1 (1993).

[8] J.C. Rose, and C.F.L. Kruppe "Methodical Series Model Test Results", FAST'91, Vol. 2, pp. 1129-1147 (1991).

[9] M. Ferrando, A. Scarmardella, N. Bose, P. Liu, B. and Veitch, "Performance of a Family of Surface Piercing Propellers", RINA Transaction, W283 (2001).

[10] H. Oberembt Zur Bestinnung Der Instationaren Flugelkrafte Bei Einem Propeller Mit Aus Dem Wasser Herausschlagenendfen Flugeln. Technical Report, Inst. Für Schiffbau Der Universitat Hamburg, Bericht Nr. 247. (1968).

[11] O. Furuya, "A Performance Prediction Theory for Partially Submerged Venti-

lated Propellers", 15th Symposium on Naval Hydrodynamics, Hamburg, Germany (1984).
[12] Y.L. Young, and S.A. Kinnas, "Numerical Modeling of Super Cavitating And Surface Piercing Propeller Flows" CAV (2001).
[13] M. Fernando, "Surface Piercing Propellers: State of the Art", Oceanic Engineering International, Vol. 1 (2), pp. 40-49 (1997).
[14] H. Shiba, "Air Drawing of Marine propellers", Technical Research Institute, Report (9) Tokyo:The Unyu Gijutsu kenkyujo (1953).
[15] www.it is.usddc.org.tw
[16] www.veem.com.au/marine

Received April 23, 2005
Accepted July 10, 2005